



ELSEVIER

Surface Science 331–333 (1995) 845–854

surface science

# Ultrathin metal film growth on $\text{TiO}_2(110)$ : an overview

Ulrike Diebold<sup>a,\*</sup>, Jian-Mei Pan<sup>b,1</sup>, Theodore E. Madey<sup>b</sup>

<sup>a</sup> Department of Physics, Tulane University, New Orleans, LA 70118, USA

<sup>b</sup> Department of Physics and Astronomy and Laboratory for Surface Modification, Rutgers, The State University of New Jersey, Piscataway, NJ 08855, USA

Received 20 August 1994; accepted for publication 14 December 1994

## Abstract

The interface between an oxide substrate and a metal overlayer may crucially influence the macroscopic behavior of technological devices such as sensors, catalysts, ceramics, and semiconductor chips. Hence investigations of adsorption, nucleation and growth of ultrathin metal films on metal oxide surfaces have attracted increasing interest during recent years. Experimental results on the growth of metal overlayers on a model oxide,  $\text{TiO}_2(110)$ , are reviewed. The emphasis is on the very initial stages of overlayer growth and on extracting general trends on metal/metal-oxide interaction by comparing results from different metal overlayers. The electronic and geometric structure, growth mode, interface formation, and thermal stability of metal films are discussed. The strength of the oxidation/reduction reaction at the interface, the wetting ability and the tendency to form a disordered layer are all related to the reactivity of the overlayer metal towards oxygen. We propose that 'reactive adsorption' accounts for the observed trends.

**Keywords:** Chromium; Copper; Growth; Hafnium; Iron; Low energy ion scattering (LEIS); Low index single crystal surfaces; Metal–insulator interfaces; Metal–metal oxide interfaces; Metal–oxide heterostructures; Titanium oxide; Wetting; X-ray photoelectron spectroscopy

## 1. Introduction

$\text{TiO}_2$  and metal-promoted  $\text{TiO}_2$  are of use in an extremely wide variety of applications. These range from the photolysis of water on  $\text{TiO}_2$  electrodes [1] and photo-oxidation of organic molecules in aqueous solutions [2], to gas sensors [3], electrocatalysis, and catalytic gas-phase conversion of molecules [4]. Naturally, this manifold of applications has stimulated a

large number of surface science investigations undertaken to obtain a better understanding of this material and its relation to technologically interesting processes and effects [5]. Additionally,  $\text{TiO}_2$  is a convenient material to work with for experimentalists. A stoichiometric, well-ordered surface can reproducibly be prepared on top of a slightly reduced single crystal [6]. The reduced bulk is n-type semiconducting, hence no charging problems occur during spectroscopic measurements.

For the above reasons,  $\text{TiO}_2$  represents the ideal model substrate for metal growth studies and a large body of work has been published addressing metals on  $\text{TiO}_2$ . We feel that a 'big picture' has started to emerge from all these investigations, with general

\* Corresponding author. Fax: +1 504 862 8702, E-mail: diebold@mailhost.tcs.tulane.edu.

<sup>1</sup> Current address: Department of Chemical Engineering, University of California at Santa Barbara, CA, USA.

trends governing certain aspects of metal/ $\text{TiO}_2$  interaction. This review on metal growth on well-characterized  $\text{TiO}_2$  surfaces attempts to summarize this. We limit ourselves to several aspects of metal/ $\text{TiO}_2$  interactions: We discuss work on only one surface; the stoichiometric, well-ordered  $\text{TiO}_2(110)$  face. We neglect the large body of literature on oxidized Ti films and powder materials, although results from such studies indicate that the general conclusions drawn from single-crystal studies may be directly applicable to these less well-defined systems. We concentrate on the very initial stage of overlayer growth, up to a film thickness of several monolayers. After a brief summary of the properties of the clean surface we discuss experimental results on the formation of the metal/ $\text{TiO}_2$  interface, the growth morphology of the films, the geometric structure and the thermal stability of the overlayers. In order to extract general trends, the emphasis is on the similarity between different overlayer metals rather than on the specifics of particular systems; the reader is referred to the original literature for many of the interesting details. The authors want to point out that this short paper is not intended to give a comprehensive review on the literature published on metals/ $\text{TiO}_2$ ; we refer only to selected articles, and the interpretations of results given in the original works are not always adopted.

## 2. The substrate: rutile $\text{TiO}_2(110)$

The (110) face of  $\text{TiO}_2$  rutile crystals is the charge-neutral, stable surface. Fig. 1 shows the top view of a ball model of this surface as has been suggested by Henrich and Kurtz [7]. The oxygen atoms drawn in white are protruding from the surface plane; these so-called ‘bridging oxygen’ rows have been speculated to act as nucleation sites during metal film growth as discussed below. Most LEED studies show an unreconstructed  $(1 \times 1)$  surface. Heating to higher temperature may produce  $(1 \times n)$  structures [8] that have been explained by missing bridging oxygen rows. No quantitative LEED  $I$ - $V$  studies have been performed so far; a medium electron energy diffraction investigation (MEED) is consistent with a surface as depicted in Fig. 1 [9]. Only very recently, STM images with atomic resolution

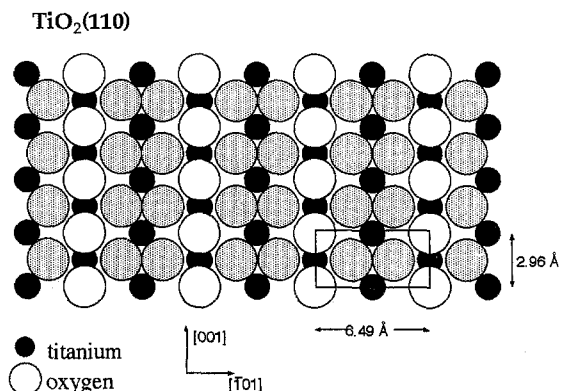


Fig. 1. Ball model of the clean, stoichiometric  $\text{TiO}_2(110)$  surface as proposed by Henrich and Kurtz [7]. The shaded circles represent in-plane oxygen atoms, the open circles the ‘bridging oxygen’ rows.

have been reported [10–12]. These studies show the dramatic influence of different preparation methods on the atomic geometry of  $\text{TiO}_2(110)$ ; but images consistent with the  $(1 \times 1)$  structure have also been observed [10]. The formation of various surface structures is to be expected for a ‘reducible’ transition metal oxide, i.e., an oxide that is stable in several oxidation states [5,13].

In the ideal, stoichiometric configuration, all Ti atoms are formally in their  $4+$  oxidation state and all oxygen atoms are present as  $\text{O}^{2-}$ . For oxide surfaces, geometric and electronic defect structures are closely related. This is exemplified in Fig. 2. The valence band region of a ‘nearly perfect’ surface shows no emission in the band gap region (Fig. 2a).

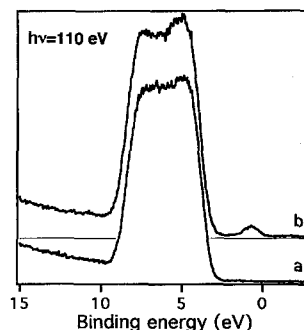


Fig. 2. Photoemission from the valence band of (a) stoichiometric  $\text{TiO}_2(110)$  and (b) after irradiation with 3 keV electrons. The spectra are taken with a photon energy of 110 eV.

Introducing surface defects creates electronic states in the band gap. For the spectrum shown in Fig. 2b, oxygen vacancies were created by electron-stimulated desorption. The corresponding Ti core-level spectra exhibit the presence of reduced  $\text{Ti}^{3+}$  states (not shown).

### 3. Metal overlayers on $\text{TiO}_2(110)$

Table 1 summarizes the main results for metal/ $\text{TiO}_2(110)$  overlayer experiments performed by the Rutgers group and by others. The film deposition experiments have been performed at low tempera-

Table 1  
Metal overlayers on  $\text{TiO}_2(110)$

Metal	Interfacial interaction	Growth morphology (method)	Geometry	Thermal stability	Ref.
Na	Reduced $\text{TiO}_x$ Formation of $\text{Na}_2\text{O}$ units	Layer growth (AES)	$c(4 \times 2)$ at 0.5 ML		[27]
K	Strongly reduced $\text{TiO}_x$ multilayers of $\text{K}_2\text{O}$ No metallic K up to high coverages		Disorder	$\text{K}_2\text{O}$ stable against annealing	[18]
Al	Strongly reduced $\text{TiO}_x$ Oxidized Al at the interface Metallic Al at higher coverages		Disorder partly reoxidation of $\text{TiO}_x$	Formation of $\text{Al}_2\text{O}_3$ at 800 K	[37]
Ti	4 Å of Ti deposition forms $\sim 12$ Å of reduced $\text{TiO}_x$ Metallic Ti at higher coverages	Formation of reduced interface, metallic clusters (LEIS)	Disorder	Onset of oxidation at 800 K	[17,47]
Hf	Strongly reduced $\text{TiO}_x$ Formation of $\text{Hf}^{4+}$ Metallic Hf at higher coverages	First layer of $\text{HfO}_2$ covers substrate (LEIS)	Disorder	Complete oxidation of Hf partly reoxidation of $\text{TiO}_x$	[16]
V	Reduced $\text{TiO}_x$ Formation of oxidized $\text{V}^{2+}$ or $\text{V}^{3+}$		Disorder	Diffusion into substrate	[35]
Cr	Reduced $\text{TiO}_x$  Formation of oxidized $\text{Cr}^{x+}$ Metallic Cr at higher coverages	Flat 2D islands,  incomplete wetting (LEIS)	$\text{Cr}(100)$  (thickness $> 10$ Å)	Clustering of metallic Cr, followed by oxidation; bulk diffusion of interfacial Cr	[15]
Mn	Reduced $\text{TiO}_x$ Formation of oxidized $\text{Mn}^{2+}$ Metallic Mn at higher coverages			Desorption/formation of $\text{MnTiO}_x$ surface layer	[36]
Fe	Slightly reduced $\text{TiO}_x$ Formation of oxidized $\text{Fe}^{2+}$ Metallic Fe at higher coverages	3D flat islands (LEIS)	$\text{Fe}(100)$ (thickness $> 10$ Å)	Encapsulation	[14,32,48]
Rh	Metallic Rh	3D islands (STM)		Encapsulation	[19,20]
Ni	No reduction of $\text{TiO}_2$ Metallic Ni		$\text{Ni}(111)$ and tilted $\text{Ni}(111)$	Encapsulation	[29,34,49]
Pd	No reduction of $\text{TiO}_2$ Metallic Pd	3D islands (LEIS)	$\text{Pd}(111)$	Encapsulation	[26]
Pt	No reduction of $\text{TiO}_2$ Metallic Pt	3D islands (LEIS)	$\text{Pt}(111)$ , 2 domains	Encapsulation	[23,33]
Cu	No reduction of $\text{TiO}_2$ Metallic Cu	3D islands (LEIS)	$\text{Cu}(111)$ , 2 domains	Strong tendency for clustering, even at low temperatures	[8,21]

IA																										VIIA																																					
H		He												Ne												Ar																																					
Li		Be												B		C		N		O		F		Ne																																							
Na		Mg		Al		Si		P		S		Cl		Ar		K		Ca		Sc		Ti		V		Cr		Mn		Fe		Co		Ni		Cu		Zn		Ga		Ge		As		Se		Br		Kr													
Rb		Sr		Y		Zr		Nb		Mo		Tc		Ru		Rh		Pd		Ag		Cd		In		Sn		Sb		Te		I		Xe																													
Cs		Ba		La		Ce		Pr		Nd		Pm		Sm		Eu		Gd		Tb		Dy		Ho		Er		Tm		Yb		Lu		Hf		Ta		W		Re		Os		Ir		Pt		Au		Hg		Tl		Pb		Bi		Po		At		Rn	

Table 2

Thickness of the reduced  $\text{TiO}_x$  layer at the metal/ $\text{TiO}_2$  interface for different metal overlayers as determined with XPS. The values for heat of formation per metal–oxygen bond are from Ref. [46].

	Heat of formation (eV)	Reduced Ti (ML)
TiO <sub>2</sub>	-5.2	
Hf/TiO <sub>2</sub>	-5.8	~ 4
Cr/TiO <sub>2</sub>	-3.1 to -4.0	~ 1
Fe/TiO <sub>2</sub>	-2.8	~ 0.4
Cu/TiO <sub>2</sub>	-1.7	~ 0

tures, mostly around room temperature, and the starting point is always a clean, stoichiometric  $\text{TiO}_2(110)$  surface. We find it useful to resort to the periodic table (Fig. 3) as a guideline for the trends that govern the aspects of overlayer growth considered here. The results quoted in Table 1 are ordered by group number of the overlayer metal; note that the more reactive metals are listed towards the top and the less reactive metals towards the bottom of the table.

### 3.1. Interfacial reactions and electronic structure

Most of the information gathered in the first category of Table 1 has been obtained by photoelectron spectroscopy methods. Fig. 4 shows representative XPS spectra of the Ti 2p region before and after deposition of small amounts of various overlayer

metals. The shape of the sharp features that are typical for the  $\text{Ti}^{4+}$  states is not altered by Cu deposition. Fe, Cr and Hf induce the formation of lower oxidation states ( $\text{Ti}^{x+}$ ,  $x < 4$ ) that give rise to low-binding energy shoulders in the XPS spectra. In Table 1 the latter is referred to as formation of a reduced  $\text{TiO}_x$  layer.

The amount of substrate reduction depends on the overlayer metal. For the examples shown in Fig. 4, a quantitative estimate of the thickness of the disturbed layer is given in Table 2. The reduction is absent for Cu and next weakest for Fe, where approximately half of surface titanium atoms are converted into the  $3+$  state [14]. Deposition of Cr affects all Ti atoms in the topmost surface layer and reduction up to  $\text{Ti}^{2+}$  is observed [15]. For Hf, the reduced region is estimated to reach approximately 4 layers into the

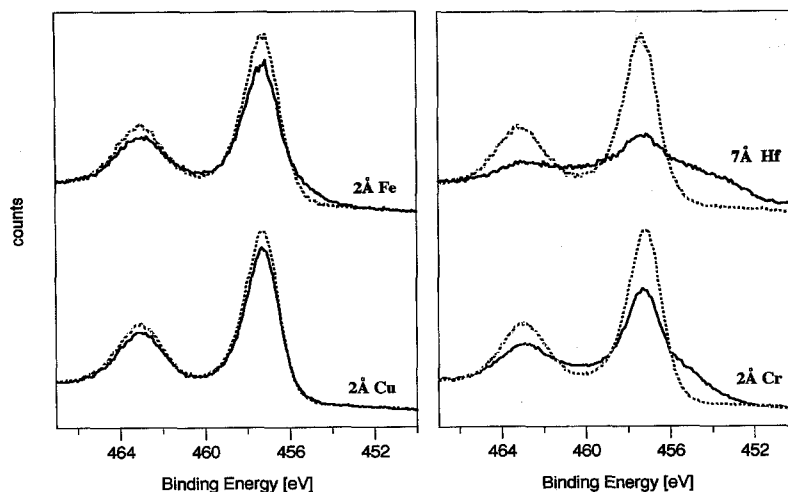


Fig. 4. XPS spectra of the Ti 2p region. Dotted lines and full lines show the Ti 2p peaks before and after metal deposition, respectively. The data are taken with Al K $\alpha$  radiation.

bulk [16]; we refer to this heavily disturbed interface as formation of a ‘strongly reduced’  $\text{TiO}_x$  layer. Only few groups have quantified the thickness of the altered  $\text{TiO}_x$  layer in this manner and the peak fitting routines needed to determine the exact number of oxidation states are not unambiguous [17]. From Table 1 the general trend is quite clear: *Formation of reduced  $\text{TiO}_x$  layers at the interface occurs upon adsorption of reactive metals.*

In the following discussion, the terms ‘reactive’ and ‘non-reactive’ metals will be used rather casually in a qualitative sense. The heat of formation per metal–oxygen bond in bulk oxides may be taken as a parameter for overlayer metal reactivity (see Table 2), but bulk thermochemical heats act only as a guideline for the reactivity of the metal/oxide interface. Qualitatively, the heat of formation correlates with the strength of the reduction reaction at the interface, with very strong interaction for Group IVa (Al in Group IIIB is also a very reactive metal) and weaker interaction for reactive metals further to the right in the periodic table.

Concurrent with substrate reduction, oxidized states are observed for reactive overlayer metals. For most of the reactive overlayer metals, the film becomes metallic above a certain thickness. The thickness of this oxidized overlayer depends on the energetics of the systems, but kinetic aspects are also important as we discuss in Section 3.4. For the reactive metal K,  $\text{K}_2\text{O}$  is observed up to very high coverages [18]. Similarly, deposition of only 4 Å of Ti results in formation of a 12 Å thick  $\text{TiO}_x$  film [17].

The borderline for this oxidation/reduction reaction at the interface appears to be the Fe group; no reduction of  $\text{TiO}_2$  has been reported for Rh [19,20], and for other metal overlayers to the right of this column. The XPS peak shape of these ‘non-reactive’ metal overlayers resembles metallic features. For very low coverages, typically well below one equivalent monolayer, a shift to higher binding energies of less than 1 eV is observed for core-level photoemission from Cu [21,22], Pt [23], and Rh [19]. As shown in Table 1, these overlayers grow in three-dimensional islands. As an explanation for this peak shift we invoke incomplete screening of the final state of the photoemission event in the small metallic clusters that are present at low coverages.

### 3.2. Growth morphology

Many growth mode studies have been published based on breaks in the AES signals during metal overlayer deposition experiments as described by Argile and Rhead [24]. Experience from our own work shows that even in cases where a very clear cluster growth is observed with other methods, analysis of AES breaks may possibly lead to erroneous assignments of the growth mode. As shown in the previous section, the electronic structure of both substrate and overlayer may change during a deposition experiment. This in turn may influence the line shape of AES peaks and complicate growth mode assignments. Hence some of the conclusions concerning growth modes given in the original references have not been included in this review. In the literature dealing with growth on metals on oxides, the nomenclature for equilibrium growth is widely used; i.e., Frank–van der Merwe (FM) for layer-by-layer growth, Stranski–Krastanov (SK) for layer followed by 3D islands and Volmer–Weber (VW) for 3D island growth. It needs to be pointed out that the studies considered here have been performed far from thermodynamic equilibrium, and, for special cases, the conventional assignment of growth modes may not be applicable for metal/ $\text{TiO}_2$  growth at all (see Section 3.4).

In Table 1, we have specified the method used for determination of the growth mode. Low-energy ion scattering (LEIS) proves to be very valuable in this respect. Due to the high surface sensitivity of this technique, only the top-most layer of a surface is probed. Provided that an independent total coverage determination can be performed, the wetting ability of a metal overlayer can be determined from the behavior of the substrate signal in its dependence on the total material deposited. This allows a clear distinction between growth modes where one full layer is formed initially (Stranski–Krastanov or Frank–van der Merwe) and the formation of three-dimensional clusters (Volmer–Weber). Fig. 5 shows the case of a reactive overlayer, Hf on  $\text{TiO}_2$ , where strong oxidation/reduction reaction is observed with XPS (Fig. 4). The titanium LEIS signal, normalized to one for a clean surface, decreases rapidly with metal coverage and reaches zero at a Hf thickness roughly equivalent to one monolayer. Correspond-

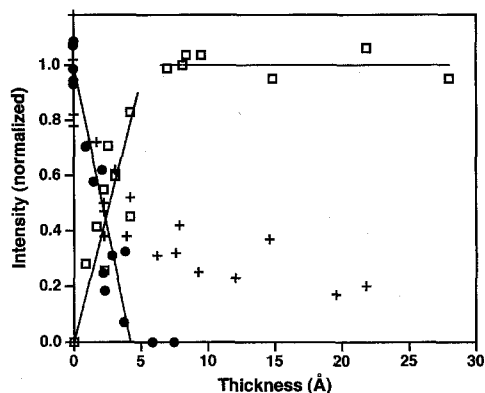


Fig. 5. Intensity of Ti (closed circles), Hf (squares) and O (crosses) signals from low energy ion scattering spectra for various Hf coverages on stoichiometric  $\text{TiO}_2(110)$  at room temperature. Substrate intensities are normalized by the value of the uncovered  $\text{TiO}_2$  surface, and Hf intensities by the value of a thick overlayer.

ingly, the Hf signal increases initially and saturates; the behavior of both signals can be fitted using straight lines as is expected for complete wetting of the first monolayer. These data clearly show that no intermixing of Hf and Ti occurs upon deposition. The oxygen LEIS signal indicates a more complex behavior; oxygen stays visible up to fairly high coverages. Incorporation of oxygen into the reactive metal overlayer is consistent with the observation that a relatively high coverage is needed before metallic Hf is seen [16].

The situation is strikingly different for Cu, where a substantial Ti signal is seen up to coverages as high as 20 Å (Fig. 6) [25]. The normalized oxygen signal follows the behavior of the Ti signal. This is clear evidence for three-dimensional island growth for this non-reactive metal. LEIS results on  $\text{Pt/TiO}_2(110)$  [23] and  $\text{Pd/TiO}_2(110)$  [26] also show cluster growth, as is the case for a combined STM/AES study on  $\text{Rh/TiO}_2(001)$  [20]. In the previous section these metals have been classified as 'non-reactive' in the sense that no oxidation/reduction reaction occurs at the interface.

The wetting ability of some metal overlayers as probed with LEIS is shown in Fig. 7. In each case, the starting point is a clean, well-ordered stoichiometric surface; the lines shown are fitted to Ti LEIS data from several separate deposition runs. The mor-

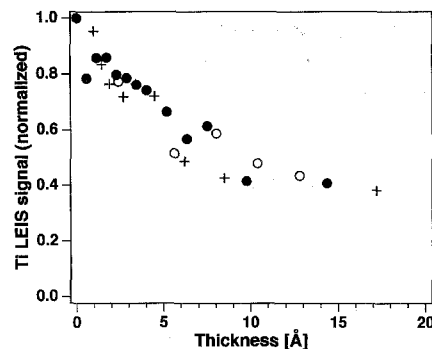


Fig. 6. Intensity of the low-energy ion scattering signal of Ti for various Cu coverages on  $\text{TiO}_2$ . The signal is normalized by the value of the uncovered  $\text{TiO}_2$  surface.

phology during the very initial stages of overlayer growth is depicted in Fig. 7. Similar to Cu, Fe grows in three-dimensional islands but it covers the surface better than the less reactive Cu overlayer. The growth of Cr is discussed in some detail in Ref. [15]. Initially, two-dimensional island formation is observed and the signal follows the trend for Hf overlayers. The deviation from the linear decrease coincides with formation of a full ML of reduced  $\text{TiO}_2$ .

Note that the wetting ability of these metals correlates well with the strength of the oxidation/reduction reaction observed with XPS (Fig. 4 and Table 2). The results on non-reactive and reactive metals give us confidence to generalize these results: *For metals with a high reactivity towards oxygen, where a strong oxidation / reduction reaction can take place*

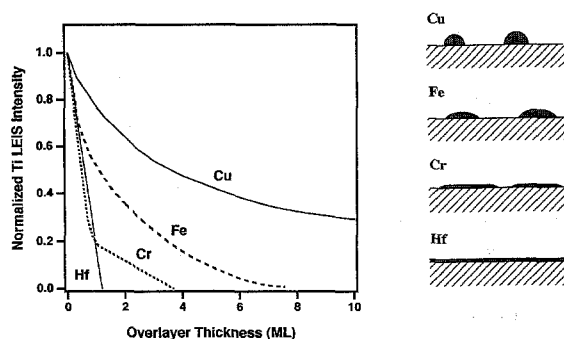


Fig. 7. Trends for attenuation of Ti LEIS signals by Cu, Fe, Cr and Hf overlayers on  $\text{TiO}_2(110)$  and schematic drawing of initial stages of film growth for Cu (three-dimensional clusters), Fe (flat islands), Cr (two-dimensional islands followed by three-dimensional growth) and Hf (formation of continuous overlayer).

*at the interface, we expect a high wetting ability for the first monolayer. Conversely, low wetting ability and agglomeration in three-dimensional islands takes place for less reactive metals that have weak interaction with the TiO<sub>2</sub> substrate.*

### 3.3. Geometry of the overlayers

For most reports, LEED has been used to study the geometry of the metal overlayers. Long-range order is a necessity for LEED and in the case of cluster growth this may not always be provided. A weakening or disappearance of a LEED pattern may not necessarily indicate disorder at a surface. In several studies, electron scattering techniques that probe short-range order have been used such as ARXPS or MEED (medium energy electron diffraction). So far, no STM studies on metals/TiO<sub>2</sub> have been reported that would exhibit good enough resolution for a direct mapping of overlayer geometries.

By inspecting Table 1 it becomes clear that very reactive overlayers tend to produce disordered films. This is indicated by the absence of long-range order (no LEED pattern) for all of the metals left of Cr, and probably also lack of short-range order. The latter has been confirmed for Hf [16] and Ti [17]. The only exception is Na, where a  $c(4 \times 2)$  superstructure has been reported for a coverage of 0.5 monolayers. Formation of Na<sub>2</sub>O dimer rows has been proposed to explain the observed LEED pattern [27].

For less reactive layers (to the right of Cr), ordered structures are seen. Relatively thick layers on the order of several equivalent monolayers are needed before ordering is observed. The bcc metals Cr and Fe exhibit a (100) orientation for films thicker than  $\sim 10$  Å. The substrate determines the azimuthal orientation of these films with the [010] direction of Fe and Cr being parallel to the [001] direction of TiO<sub>2</sub> [28].

The most densely packed (111) surface is formed by the non-reactive fcc metals Cu, Ni, Pd and Pt. Again, some registry with the substrate is observed; Cu atoms are placed in registry with the  $[\bar{1}\bar{1}0]$  direction of the TiO<sub>2</sub>(110) surface [8]. Atoms in the second layer of a (111) oriented film can grow in two different orientations depending which one of

the three-fold hollow sites is occupied. Since these non-reactive overlayers have been shown or are predicted to grow in three-dimensional clusters, domains with the two possible orientations are formed as has been observed for Cu [28] and Pt [23]. For Ni, two different types of islands have been seen; hexagonal structures oriented parallel to the surface and inclined to the surface plane [29].

Nucleation along the bridging oxygen rows has been invoked for the formation of these ordered structures. Indirect evidence for such behavior has been given by resonant photoemission experiments for Fe/TiO<sub>2</sub>(110) [30] and by LEED in the case of Na/TiO<sub>2</sub> [27]. TEM images show one-dimensional rows for Rh/TiO<sub>2</sub> [31], the system investigated had been prepared by wet impregnation, however. A direct determination of the role of the bridging oxygen rows in the nucleation of metal overlayers during metal vapor deposition in an UHV environment is still missing.

### 3.4. Thermal stability of overlayers

The behavior of thin metal films on TiO<sub>2</sub>(110) during annealing excursions is richer and complex, yet categorizing the overlayer metals by their reactivity is useful for grouping metals with similar behavior. We start our discussion with Cu at the right side of the periodic table. Pronounced clustering behavior with formation of bigger clusters from smaller ones occurs upon annealing [25]. Changes in XPS signals are observed at substrate temperatures as low as 160 K. This strong tendency for clustering is attributed to the very weak interaction with the substrate.

For Group VIII metals, encapsulation of metallic clusters with a reduced TiO<sub>x</sub> overlayer is observed upon annealing to temperatures of several hundred K [19,32–34]. This ‘decoration’ effect is related to the catalytically very active SMSI (strong metal support interaction) state [4], and has long represented a challenge for the surface science and the catalysis communities.

When going further to the left in the periodic table (Group Va–VIIa), a behavior evolves that can be summarized as formation of ternary oxides, limited by kinetic effects. V diffuses into the bulk [35] as does Cr [15]; the latter shows a concurrent tendency for agglomeration in metallic clusters, fol-

lowed by oxidation. Mn is a somewhat exceptional case; it exhibits a very low cohesive energy so that desorption takes place at relatively low temperatures. The residue of this desorption process appears to be a ternary  $\text{MnTiO}_x$  surface oxide [36].

Let us now consider the most reactive overlayers, where several oxidized layers are produced already for metal deposition at low temperature. Upon heating, more oxygen tends to be extracted from the substrate. A sharp onset of oxygen migration around 800 K is observed for annealing of a Ti layer on  $\text{TiO}_2(110)$  [17], and a stoichiometric, ordered  $\text{TiO}_2$  surface is restored. Oxidation of the metallic component of the films is observed for Hf [16], Cr [15] and Al [37]. The multilayers of  $\text{K}_2\text{O}$  that are produced directly upon deposition are stable against heating [18]. None of these films order during annealing. The reduced  $\text{Ti}^{x+}$  atoms at the interface are partly re-oxidized and no indication for interdiffusion of the metal atoms of these oxide films is observed.

#### 4. Discussion

Considering the thermal stability of the metal films discussed in Section 3.4, the reason for our hesitation to speak in terms of the conventionally used equilibrium growth modes for metal film growth on  $\text{TiO}_2$  becomes evident. Clearly, interfacial reactions, interdiffusion of oxygen, ternary oxide formation and the rather remarkable encapsulation behavior cannot be categorized in conventional terms. However, an activation energy barrier has to be overcome before a massive diffusion of material at the metal/ $\text{TiO}_2$  interface starts; and for deposition at low temperatures the wetting of metal overlayers correlates well with one simple parameter – the reactivity of the overlayer metal.

We propose that ‘*reactive adsorption*’ accounts for the observed trends: When a reactive metal overlayer atom arrives at the surface, it reacts with surface oxygen atoms and strong bonds are formed. During this reaction, oxygen atoms are displaced. This means that the observed reduction of the  $\text{TiO}_x$  interface occurs via displacement of O and/or incorporation of O into the first layers of the overlayer (see Fig. 5). Remember that the geometric and electronic structures of metal oxides are closely related

(Fig. 2). The massive ‘attack’ of the surface that results in disordered overlayers for very reactive overlayers corroborates this picture (Section 3.3). Even for the reactive metal that exhibits the weakest interaction, Fe, indirect evidence for displacement of O atoms is seen [30]. The more reactive the overlayer metal, the more the ideal geometric structure of the interface will be disturbed. This also supports the suspected nucleation along bridging oxygen rows, since these rows are believed to be more reactive than in-plane oxygen.

Often, the surface free energy of the substrate and the overlayer material are considered for predictions of growth modes. The surface free energy of oxide materials is generally much lower than for metals [38]; if one considers only the surface free energy, this would imply that all metal overlayers would grow in three-dimensional islands. The apparent discrepancy must be related to the interfacial energy which is proportional to the strength of the metal/oxygen bonds. A large negative energy can be gained from interfacial bonding [14], additionally the structural changes that occur upon oxygen displacement have to be taken into account [39].

Of course, kinetic effects cannot be neglected and diffusion on the surface will contribute to the observed manifestation of growth morphology. For deposition of ‘non-reactive’ metals, no substantial displacement of oxygen takes place. Since the system tends to minimize its total energy, the overlayer grows in three-dimensional islands and kinetics determines the size, distribution and number of the clusters [21,23]. We are not aware of detailed studies on the kinetics of overlayer growth for more reactive overlayer metals.

#### 6. Conclusion, open questions and outlook

In summary, a predictive understanding is emerging for several aspects of overlayer growth on the model surface  $\text{TiO}_2(110)$ . The strength of oxidation/reduction reaction, the wetting ability of the overlayer, the tendency for developing ordered or disordered structures, and even the annealing behavior of the systems scale with the reactivity of the overlayer metal. Several questions remain still open. One is how the reactive adsorption of the overlayer



metal actually takes place. Direct structural probes such as STM may be of help in addressing issues like adsorption sites of the metals; the recent success in obtaining atomically resolved images on  $\text{TiO}_2$  gives rise for hope in this direction. Theoretical calculations of metal overlayers on  $\text{TiO}_2$  are needed, very detailed theoretical investigations on clean  $\text{TiO}_2$  surfaces and of defect structures exist already [40–43]. Together with the systematics obtained from experimental results such calculations on metal adsorption should be quite powerful for obtaining deeper insight in these systems.

The main open question of course is: Can the trends observed for metal overlayer growth on  $\text{TiO}_2$  be extrapolated to other oxide substrates? A surface science investigation by Peden et al. [44] has shown a correlation between wetting tendency and metal reactivity on oxidized tungsten surfaces. The correlation between good wetting and bonding and metal reactivity that is well-known to ceramists also points in this direction [45]. From the results on  $\text{TiO}_2$  surfaces it appears that ‘reducibility’, i.e., the stability of the oxide substrate in several oxidation states, is an important factor for the observed trends. Several transition metal oxides fall into the category of reducible metal oxide surfaces [13], and we feel that similar behavior is likely for metal overlayer growth on these materials. The non-reducible oxides  $\text{MgO}$  and  $\text{Al}_2\text{O}_3$  are of major interest for technical applications. Quite a large number of metal overlayer studies have been performed on these substrates. To our knowledge no such a clear, systematic trends have been established for these systems on an atomistic scale; only further systematic investigations in this direction will prove if a general picture for metal on metal oxide growth can be established.

## Acknowledgments

This work has been supported in part by NSF grant DMR-8907553 to Rutgers University. The help of Lizhong Zhang and Dr. Hui-Shu Tao in data taking is acknowledged. U.D. thanks the Tulane Committee on Research Summer Fellowship and the Louisiana Education Quality Support Fund for partial support of this work.

## References

- [1] A. Fujishima and K. Honda, *Nature* 238 (1972) 37.
- [2] M. Grätzel, *MRS Bull.* October (1993) 61.
- [3] K.D. Schierbaum, X. Wei-Xing, S. Fischer and W. Göpel, in: *Adsorption on Ordered Surfaces of Ionic Solids and Thin Films*, Eds. E. Umbach and H.J. Freund (Springer, Berlin, 1993) p. 268.
- [4] G.L. Haller and D.E. Resasco, *Advan. Catal.* 36 (1989) 173.
- [5] V.E. Henrich and P.A. Cox, *The Surface Science of Metal Oxides* (Cambridge Univ. Press, Cambridge, 1994).
- [6] J.-M. Pan, B.L. Maschhoff, U. Diebold and T.E. Madey, *J. Vac. Sci. Technol. A* 10 (1992) 2470.
- [7] V.E. Henrich and R.L. Kurtz, *Phys. Rev. B* 23 (1981) 6280.
- [8] M.-C. Wu and P.J. Møller, *Surf. Sci.* 224 (1989) 265.
- [9] B.L. Maschhoff, J.-M. Pan and T.E. Madey, *Surf. Sci.* 259 (1991) 190.
- [10] D. Novak, E. Garfunkel and T. Gustafsson, *Phys. Rev. B* 50 (1994) 5000.
- [11] H. Onishi and Y. Iwasawa, *Surf. Sci.* 313 (1994) L783.
- [12] M. Sander and T. Engel, *Surf. Sci.* 302 (1994) L263.
- [13] G.V. Samsonov, *The Oxide Handbook* (IFI/Plenum, New York, 1982).
- [14] J.-M. Pan and T.E. Madey, *J. Vac. Sci. Technol. A* 11 (1993) 1667.
- [15] J.-M. Pan, U. Diebold, L. Zhang and T.E. Madey, *Surf. Sci.* (1993) 411.
- [16] L. Zhang, U. Diebold, J.-M. Pan and T.E. Madey, to be published.
- [17] J. Mayer, E. Garfunkel, T.E. Madey and U. Diebold, *J. Electron Spectrosc. Relat. Phenom.*, in press.
- [18] R.J. Lad and L.S. Dake, *Proc. Mater. Res. Soc.* 238 (1992) 823.
- [19] H.R. Sadhegi, *Appl. Surf. Sci.* 19 (1984) 330.
- [20] G. Poirier, B.K. Hance and J.M. White, *J. Phys. Chem.* 97 (1993) 6500.
- [21] U. Diebold, J.-M. Pan and T.E. Madey, *Surf. Sci.* 287/288 (1993) 896.
- [22] M.-C. Wu and P.J. Møller, *Surf. Sci.* 224 (1989) 250.
- [23] H.-P. Steinrück, F. Pesty, L. Zhang and T.E. Madey, *Phys. Rev. B* 51 (1995) 2427.
- [24] C. Argile and G.E. Rhead, *Surf. Sci. Rep.* 10 (1989) 277.
- [25] U. Diebold, J.-M. Pan and T.E. Madey, *Phys. Rev. B* 47 (1993) 3868.
- [26] L. Zhang and T.E. Madey, unpublished.
- [27] H. Onishi, T. Aruga, C. Egawa and Y. Iwasawa, *Surf. Sci.* 199 (1988) 54.
- [28] J.-M. Pan, B.L. Maschhoff, U. Diebold and T.E. Madey, *Surf. Sci.* 291 (1993) 381.
- [29] M.-C. Wu and P.J. Møller, in: *The Structure of Surfaces III*, Eds. S.Y. Tong, M.A.V. Hove, X. Xide and K. Takanayagi (Springer, Berlin, 1993).
- [30] U. Diebold, H.-S. Tao, N.D. Shinn and T.E. Madey, *Phys. Rev. B* 50 (1994) 14474.
- [31] S. Fuentes, A. Vazquez, J.G. Perez and M.J. Yacman, *J. Catal.* 99 (1986) 492.

- [32] J.-M. Pan and T.E. Madey, *Catal. Lett.* 20 (1993) 269.
- [33] D.J. Dwyer, J.L. Robbins, S.D. Cameron, N. Dudash and J. Hardenbergh, in: *Strong Metal-Support Interactions*, Eds. R.T.K. Baker, S.J. Tauster and J.A. Dumesic (American Chemical Society, Washington, DC, 1986).
- [34] C.C. Kao, S.C. Tai, M.K. Bahl, Y.W. Chung and W.J. Lo, *Surf. Sci.* 95 (1980) 1.
- [35] Z. Zhang and V.E. Henrich, *Surf. Sci.* 235 (1992) 263.
- [36] U. Diebold and N.D. Shinn, in preparation.
- [37] L.S. Dake and R.J. Lad, *Surf. Sci.* 289 (1993) 297.
- [38] S.H. Overbury, P.A. Bertrand and G.A. Somorjai, *Chem. Rev.* 75 (1975) 547.
- [39] M. Weinert, R.E. Watson, J.W. Davenport and G.W. Fernando, *Phys. Rev. B* 39 (1989) 12585.
- [40] S. Munnix and M. Schmeits, *Phys. Rev. B.* 30 (1984) 2202.
- [41] S. Munnix and M. Schmeits, *Phys. Rev. B.* 31 (1985) 3369.
- [42] M. Ramamoorthy, D. Vanderbilt and R.D. King-Smith, *Phys. Rev. B* 49 (1994) 16721.
- [43] M. Ramamoorthy, R.D. King-Smith and D. Vanderbilt, *Phys. Rev. B* 49 (1994) 7709.
- [44] C.H.F. Peden, K.B. Kidd and N.D. Shinn, *J. Vac. Sci. Technol. A* 9 (1991) 1518.
- [45] K.C. Russel, S.-Y. Oh and A. Figueriedo, *MRS Bull.* 46 (1991).
- [46] R.C. Weast, M.J. Astle and W.H. Beyer, *CRC Handbook of Chemistry and Physics* (1988–1989).
- [47] G. Rocker and W. Göpel, *Surf. Sci.* 181 (1987) 530.
- [48] J. Deng, D. Wang, X. Wei, R. Zhai and H. Wang, *Surf. Sci.* 249 (1991) 213.
- [49] H. Onishi, T. Aruga, C. Egawa and Y. Iwasawa, *Surf. Sci.* 223 (1990) 261.